Optimal Source Tracking and Beaming of LISA

Archana Pai

Max-Planck Institut für Gravitationsphysik, Am Mühlenberg 1, 14476 Potsdam, Germany

Abstract. We revisit the directionally optimal data streams of LISA first introduced in Nayak etal. It was shown that by using appropriate choice of Time delay interferometric (TDI) combinations, a monochromatic fixed source in the barycentric frame can be optimally tracked in the LISA frame. In this work, we study the beaming properties of these optimal streams. We show that all the three streams $v_{+,\times,0}$ with maximum, minimum and zero directional SNR are highly beamed. We study in detail the frequency dependence of the beaming.

Keywords: gravitational waves —data analysis—TDI
PACS: 95.55.Ym, 04.80.Nn, 95.75.Wx

1. INTRODUCTION

The space-based gravitational wave (GW) mission LISA [1] —Laser Interferometric Space Antenna —consists of three identical space-crafts forming an equilateral triangle of side 5×10^6 km following heliocentric orbit trailing the Earth by 20°. The plane of LISA makes an angle of 60° with the plane of the ecliptic. Each space-craft completes one orbit around the sun as well as in LISA plane in one year. The mission is aimed at detecting and analyzing the low frequency GW signals in the frequency range of 0.1mHz – 1Hz. The astrophysical sources for the LISA include galactic binaries, super-massive black-holes (BH), extreme mass ratio inspirals, intermediate mass BHs.

Due to LISA's rotational as well as orbital motion, a fi xed source in the barycentric frame appears to follow a specifi c track in its sky. This introduces amplitude modulation, frequency modulation, and phase modulation in the 6 Doppler data streams. A large number of interferometric confi gurations, having different frequency and angular response, can be constructed from these data streams which makes LISA not just a single detector but a network of interferometers.

The choice of the combination of the data streams depend on the which question one wishes to address. In Ref. [2], we addressed the question of directional optimality in LISA i.e. for a given sky location, which LISA data stream gives maximum SNR. It was shown that the directional optimality condition gives three data streams: (1) v_+ – with maximum directional SNR, (2) $v_\times$ – with minimum directional SNR, (3) v_0 – with zero directional SNR. It was shown that the data stream v_+ optimally tracks the source motion (in the LISA sky) of a fi xed source in the barycentric frame. Here, *tracking* involves appropriate choice of data combinations (switch combinations as source moves) which gives maximum SNR in that direction. Tracking known monochromatic binaries with such streams could give information about the source distance, polarizations. For an unknown distant source, it would amount to 'looking' in a specifi c direction in a particular frequency band.

CP873, *Laser Interferometer Space Antenna—6th International LISA Symposium,*
edited by S. M. Merkowitz and J. C. Livas

In this work, we study the beaming property of the optimal data streams (in particular, v_+) for a monochromatic source tracked for a year. We show that $v_+, v_\times and v_0$ are beamed, i.e. they are sensitive towards the tracking direction. The beam-width depends on the frequency under consideration. We study the nature of this dependence.

The paper is organized as follows: In Sec 2, we review the TDI. In the fi rst half of Sec. 3, we summarize the main results of Ref.[2] pertaining to the directionally optimal TDI streams. In the later half of Sec 3, we discuss the beaming properties of the directional streams followed by conclusion in Sec. 4.

2. TDI DATA STREAMS

The 6 LISA Doppler data streams W_σ^m, where $m = 1,2,3, \sigma = \pm$, [see Fig.1[1]] are obtained by letting the laser beams from each space-craft to travel towards two other space-crafts and are beaten with the on board laser. m corresponds to the arm index and $(-)+$ indicates the laser beam traveling in the (anti-)clockwise direction.

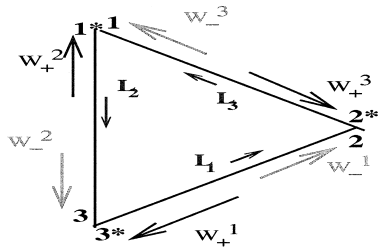

FIGURE 1. The LISA constellation

These Doppler data streams contain the phase fluctuation noise of the master laser ($\Delta\nu/\nu_0 \simeq 10^{-13}/\sqrt{Hz}$) which is several orders of magnitude higher than the LISA designed sensitivity level of $h \sim 10^{-22}$. Using TDI technique, W_σ^m can be combined by appropriately delaying them with time delay operators to construct laser noise-free data streams Ref. [3]. The TDI scheme is based on the principle of sagnac interferometry — the light-beam is split and made to travel along two paths in opposite direction of equal length which are then subtracted to remove the laser noise. In TDI, equal path difference is achieved by adding Doppler-streams with appropriate time delay operators which are then added (or subtracted) to obtain laser noise free data stream.

Any laser noise-free data combination can be written as $D = \sum_{m=1}^{3} \sum_{\sigma=\pm} \rho_{m\sigma} W_\sigma^m$, where $\rho_{m\sigma}$ are polynomials of time-delay operators $E_m : E_m C_j(t) = C_j(t - L_m)$ and C_m are the laser phase noise fluctuation at the space-craft m. The Sagnac TDI combinations $\{\alpha, \beta, \gamma, \zeta\}$ in terms of $\{\rho_{m+}, \rho_{m-}\}$ are given by [2]

$$\alpha = \{E_2, 1, E_1E_2, -E_3, -E_1E_3, -1\} \qquad \beta = \{E_2E_3, E_3, 1, -1, -E_1, -E_1E_2\}, \quad (1)$$

$$\gamma = \{1, E_1E_3, E_1, -E_2E_3, -1, -E_2\} \qquad \zeta = \{E_3, E_1, E_2, -E_2, -E_3, -E_1\}. \quad (2)$$

---

[1] $W_+^1 = U^3, W_+^2 = U^1, W_+^3 = U^2, W_-^1 = -V^2, W_-^2 = -V^3, W_-^3 = -V^1$ of [3]

[2] This set forms a generator set for an algebraic module of all laser noise free data combinations Ref. [3].

The ζ combination is termed as symmetrized sagnac due to its symmetric structure and is insensitive to GW at low frequency $f << 1/L = 60$ mHz ($L = 16.7$ sec.).

The noise vector for any combination D is given by

$$N^D = (2\sqrt{S^{pf}}(\rho^D_{m+} + \mu^D_{m+}), 2\sqrt{S^{pf}}(\rho^D_{m-} + \mu^D_{m-}), \sqrt{S^{opt}}\rho^D_{m+}, \sqrt{S^{opt}}\rho^D_{m-}) \quad (3)$$

where the polynomials $\mu_{m\pm}$ are defi ned as $\mu_{3-} = (E_3\rho_{3+} - \rho_{3-})/2 = -\mu_{2+}$. The rest $\mu_{m\sigma}$ can be obtained by cyclic permutations. The $S^{pf} = 2.5 \times 10^{-48}(f/1\text{Hz})^{-2}\text{Hz}^{-1}$ and the $S^{opt} = 1.8 \times 10^{-37}(f/1\text{Hz})^2\text{Hz}^{-1}$ are the one-sided power spectral densities (PSD) of the proof-mass noise and optical-path noise respectively [1]. In the frequency domain $E_m = \exp(i\Omega L_m)$.

For simplicity, throughout this work, we assume the three arms of LISA to be equal i.e. $L_m \equiv L$. This helps in simplifying the expressions of TDI streams and are exact for low frequencies. However for higher frequencies, the above simplifi cation leads to small discrepancies. Nevertheless, one can easily extend this for unequal-arm interferometry.

A set of TDI data streams which diagonalizes the noise covariance matrix $N^{(I)} \cdot N^*_{(J)}$ are [4]: $Y^{(1)} = (\alpha + \beta - 2\gamma)/\sqrt{6}, Y^{(2)} = (\beta - \alpha)/\sqrt{2}, Y^{(3)} = (\alpha + \beta + \gamma)/\sqrt{3}$. $Y^{(1)}, Y^{(2)}$ and $Y^{(3)}$ are known as E,A and T in the LISA literature.

3. DIRECTIONAL DATA STREAMS

As mentioned in the introduction, the three $Y^{(I)}$'s give different frequency as well as angular response. A large number of TDI data streams $\sum \alpha_{(I)}(f, \theta_L, \phi_L)Y^{(I)}$ with different angular and frequency responses can be constructed from them. The choice of a combination depends on the question one wishes to address. In Ref. [2], we asked the following question: If one wants to observe a particular sky location $\{\theta_B, \phi_B\}$, in a given frequency bin, which $\sum \alpha_{(I)}Y^{(I)}$ TDI data stream would be optimal (maximum SNR)? We fi rst briefly summarize the results of Ref. [2].

The GW response of $Y^{(I)}$ expressed in frequency domain is

$$h^{(I)}(\Omega) = F^{(I)}_+(\Omega)h_+(\Omega) + F^{(I)}_\times(\Omega)h_\times(\Omega), \quad (4)$$

where, the antenna pattern functions $F^{(I)}_{+,\times}$ in terms of the transfer function of each Doppler data stream is

$$F^{(I)}_{+,\times}(\Omega) = i\sum_{m,\sigma} \rho^{(I)}_{m\sigma}\Delta\phi_m \exp(i\Omega(\hat{w}\cdot\hat{a}_m))\,\text{Sinc}(k_{m\sigma}\Delta\phi_m)\xi_{m;+,\times}, \quad (5)$$

where $\hat{w}$ is the direction vector to the source in the LISA frame, $\Delta\phi_m = \Omega L_m/2$, $k_{m\mp} = 1 \mp \hat{w}\cdot\hat{n}$ appears in the accumulated phase due to GW oscillation as the laser travels from one space-craft to another (anti-)clockwise direction, $\hat{a}_m$ is the normal vector from LISA centre to each arm m and $\xi_{m;+\times}$ are the responses of each arm to the two GW polarizations.

The SNR maximization for a particular direction is a constrained optimization problem. The data combinations are obtained from the eigen-vectors of the SNR squared

matrix (averaged over the polarizations)

$$\rho^{(I)}_{(J)} = \left(f^{(I)}_{+} f^{*}_{+(J)} + f^{(I)}_{\times} f^{*}_{\times(J)} \right) (\Omega) \tag{6}$$

where $f^{(I)}_{+,\times} = H_0 F^{(I)}_{+,\times}/n_{(I)}$, H_0^2 is the average signal energy over the GW polarization and $n^2_{(I)}$ is the noise PSD of $Y^{(I)}$. The eigen-values are the instantaneous squared SNR for the optimal data streams. The 3 eigen vectors are given by:

$$\vec{V}_{+} \;=\; c_{+}\vec{f}_{+} + c_{\times}\vec{f}_{\times}, \quad \vec{V}_{\times} = c^{*}_{\times}\vec{f}_{+} - c_{+}\vec{f}_{\times}, \quad \vec{V}_0 = \vec{f}_{+}^{\,*} \times \vec{f}_{\times}^{\,*}, \tag{7}$$

where the coeffi cient $c_{\times} = \vec{f}_{\times}^{\,*} \cdot \vec{f}_{+}$ and

$$c_{+} = \frac{1}{2}\left[|\vec{f}_{+}|^2 - |\vec{f}_{\times}|^2 + \sqrt{(|\vec{f}_{+}|^2 - |\vec{f}_{\times}|^2)^2 + 4|\vec{f}_{+} \cdot \vec{f}_{\times}^{\,*}|^2} \right] = \mathrm{snr}^2_{+} - |\vec{f}_{\times}|^2 = -(\mathrm{snr}^2_{\times} - |\vec{f}_{+}|^2). \tag{8}$$

Note that the orthogonal pair of $\{\vec{V}_{+}, \vec{V}_{\times}\}$ is obtained by the linear combination of $\vec{f}_{+}$ and $\vec{f}_{\times}$ and hence lie in $\{\vec{f}_{+}, \vec{f}_{\times}\}$ —polarization —plane. The 2×2 matrix which transforms $\{\vec{f}_{+}, \vec{f}_{\times}\}$ to $\{\vec{V}_{+}, \vec{V}_{\times}\}$ is traceless-hermitian. Naturally, the direction orthogonal to this plane contains no signal, i.e. a data stream obtained from $\vec{V}_0$ (orthogonal to $\{\vec{f}_{+}, \vec{f}_{\times}\}$ plane) is a null stream. Hence, the triplet $\{\vec{V}_{+}, \vec{V}_{\times}, \vec{V}_0\}$ gives complete directional information of the GW signal. The tracking coeffi cients for the optimal data streams are $\alpha_{(I)+,\times,0} = V^{(I)*}_{+,\times,0}/n_{(I)}$. In summary, the data stream (i) $v_{+} \equiv \alpha_{(I)+} Y^{(I)}$ gives maximum directional SNR i. e. snr_{+}, (ii) $v_{\times} \equiv \alpha_{(I)\times} Y^{(I)}$ gives the smallest non positive SNR i. e. $\mathrm{snr}_{\times}$ and (iii) $v_0 \equiv \alpha_{(I)0} Y^{(I)}$ gives zero directional SNR. At low frequency, $c_{\times} = 0$ and v_{+} tracks the $+$ polarization while $v_{\times}$ tracks the $\times$ polarization of GW, hence their subscripts [2].

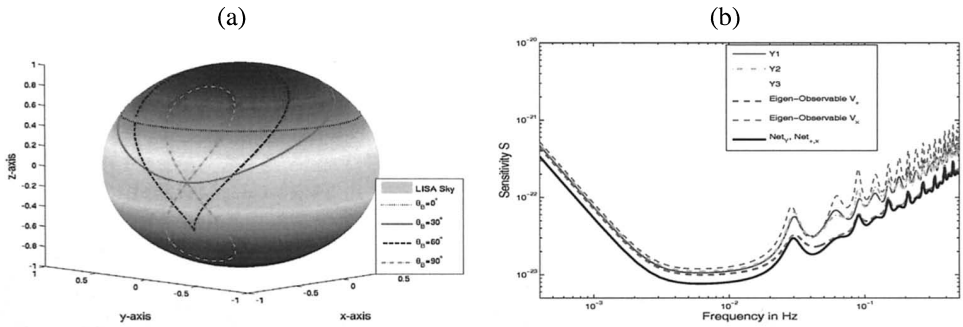

FIGURE 2. (a) Source coordinates $\{X_L(t), Y_L(t), Z_L(t)\}$ in LISA frame for a fixed source at $\phi_B = 200°$ for various θ_B. (b) LISA Sensitivity for various data streams while tracking source at $\{\theta_B, \phi_B\} = \{60°, 200°\}$ and $H_0 = 1$, $T = 1$ year.

3.1. Source tracking and Integrated SNR

Due to LISA's motion, a fi xed direction $\hat{n} = \{\theta_B, \phi_B\}$ in barycentric frame appears to follow a track $\{\theta_L(t), \phi_L(t)\}$ in LISA's sky, see Fig. 2(a). We track the direction

and obtain the integrated SNR as follows: We choose the optimal data combination pertaining to the source direction $\{\theta_L(t;\hat{n}_B),\phi_L(t;\hat{n}_B)\}$, at each time step, in LISA frame (including Doppler shift correction to the frequency). The corresponding SNR at each time-step is referred to as instantaneous SNR i.e. $\mathrm{snr}_{+,\times}$. We integrate the instantaneous SNR as given below

$$\mathrm{SNR}^2_{+,\times}(\hat{n}_B) \;=\; \int_0^T \mathrm{snr}^2_{+,\times}(\theta_L(t;\hat{n}_B),\phi_L(t;\hat{n}_B))dt\,. \tag{9}$$

The network SNR while tracking $\hat{n}_B$ over 1 year period is obtained by summing the squared integrated SNR's of the individual data streams [3]

$$\mathrm{SNR}^2_{\mathrm{Net}}(\hat{n}_B) = \mathrm{SNR}^2_{+}(\hat{n}_B) + \mathrm{SNR}^2_{\times}(\hat{n}_B) = \sum_{I=1}^{3} \mathrm{SNR}^2_{I}(\hat{n}_B)\,. \tag{10}$$

In Fig.2(b), we plot the LISA sensitivity $S = 5/\mathrm{SNR}_{\mathrm{int}}$ for a monochromatic source tracked with several data combinations. $\mathrm{SNR}_{\mathrm{int}}$ is the integrated SNR along the source track (in LISA frame) for a given combination. For switching combination, e.g. optimal streams $v_{+,\times}$, $\mathrm{SNR}_{\mathrm{int}} = \mathrm{SNR}_{+,\times}$.

Fig.2(b) displays the following features: (i) At low frequencies ($f \leq 3$ mHz), v_+, $v_\times$ have similar sensitivities and are proportional to f^{-2} (similar to $Y^{(1,2)}$); the data stream $Y^{(3)}$ ($=\zeta$) is insensitive to GW. (ii) Above 25 mHz, all $Y^{(I)}$'s become comparable in their sensitivities. The wavelength of GW (λ_{GW}) is comparable to L. This introduces geometry dependent features in the LISA sensitivity curve. For example, $Y^{(3)}$ combination is most sensitive when $f_{\mathrm{gw}} = f_L = 1/L = 60$ mHz or multiples of f_L. As v_+ contains contribution from $Y^{(I)}$, this feature also appears in its sensitivity, see Fig.3(a). The dips in the integrated SNR of v_+ correspond to the zeros of $Y^{(3)}$ (at $f = (2n-1)f_L/2$ mHz, n is a positive integer).

3.2. Beaming of Optimal Stream

Although, tracking $\hat{n}_B$ with a network comprising of $Y^{(I)}$ —Net $_Y$ —and with a network of v_+ and $v_\times$ —Net $_{+,\times}$ —gives the same integrated (as well as instantaneous) SNR [see, for instance, Eq.(10) and Fig.2(b)], we show in this section that they possess completely different beaming properties.

To demonstrate this, we divide the sky in the barycentric frame in 1 square degree patches. We observe each of this patch with the data streams $Y^{(I)}$ and integrate the squared SNR for a year along its track in the LISA frame ($H_0 = 1$). In order to perform the same exercise with v_+, $v_\times$, v_0, we choose to track an arbitrary source direction $\{\theta_B,\phi_B\} = \{60^\circ, 200^\circ\}$. In Fig. 4,5(a), contour plots of integrated squared SNR are drawn (in barycentric frame) for all the data streams. The SNR is normalized with respect to SNR_+. The observations and the implications are as follows:

---

[3] Note that $\mathrm{SNR}^2_{\mathrm{Net}}(\hat{n}_B)$ can also be obtained by summing the squared SNR's of the individual data streams (trace of $\rho^{(I)}_{(J)}$) and integrating the resultant.

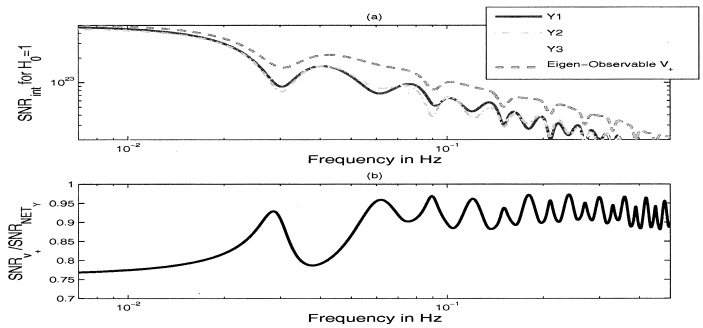

FIGURE 3. (a) SNR of v_+ and $Y^{(I)}$ *vs* f, (b) SNR $+$ /SNR$_{\rm Net}$*vs*f for tracking $\{\theta_B, \phi_B\} = \{60°, 200°\}$.

(i) The data streams v_+, $v_\times$ and v_0 are all beamed. In other words, the beam pattern of these streams peaks towards the tracking direction, whereas the $Y^{(I)}$ streams are sensitive to a large fraction of the sky; see, for instance, Fig. 4(b), 5(a). The contours of the integrated SNR while tracking a particular direction give the point spread function (psf) of the source. In the language of the GW data analysis literature, these contours can be related to the ambiguity function in the source location parameter space. The width of the psf determines the size of the template.
(ii) Net$_{+,\times}$ gives the same integrated SNR as that of Net$_Y$. However, Net$_{+,\times}$ is highly beamed as opposed to Net$_Y$. The complimentary feature of Net$_{+,\times}$ and v_0 is apparent from the bright and dark patch centered around the tracking direction [see for instance, Fig. 4(b), 5(a)]. This property can have a possible immediate application in LISA data analysis. In LISA, we expect to observe a large number of GW sources from different sky locations in nearby frequency bins. Thus, with the combination of Net$_{+,\times}$ and its complementary null stream v_0, one could systematically suppress other sky directions without compromising on SNR.
(iii) In the low frequency ($f < 10$ mHz), Net$_{+,\times}$ does not show beaming and gives the same beam pattern as that of Net$_Y$. This is because the angular response of $Y^{(1),(2)}$ is that of a single Michelson interferometer. The stream $Y^{(2)}$ differs from the $Y^{(1)}$ by 45° rotation [see [2],Fig.4 (a)] which makes the pattern azimuthal invariant after tracking. Further, the angular response of any TDI combination will be limited by the signal antenna angular pattern (size of earth's orbit $\sim \lambda_{\rm GW}$).
(iv) In Fig. 4(b) and 5(a), v_+ and Net$_{+,\times}$ are beamed along the tracking direction $\{60°, 200°\}$. At 50 mHz (being closer to $f \sim f_L$) , as opposed to at 25 mHz, $Y^{(3)}$ is more sensitive compared to $Y^{(1),(2)}$.

One would expect that beam-width of the optimal streams is a monotonically decreasing function of frequency. However, we fi nd super-imposed oscillations on the monotonically decreasing behavior in the beam-width[see, Figs. 5(b),6][4]. Below, we summarise

[4] In order to test this, we choose v_+ (maximum SNR) to track the source at different frequencies. This is because, it is shown in Fig.3(b),, for $f > 25$ mHz, v_+ contributes more than 80% to Net$_{+,\times}$.

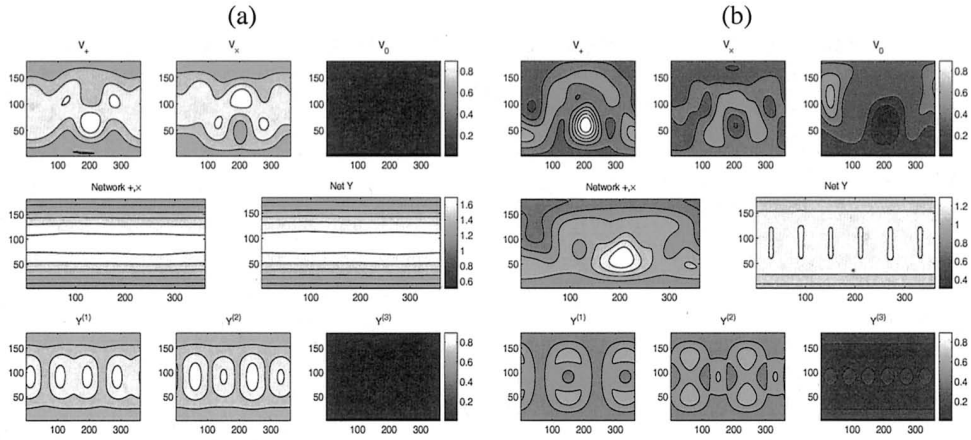

FIGURE 4. Integrated squared SNR at (a) $f = 10$ mHz, (b) $f = 25$ mHz and tracking $\{\theta_B, \phi_B\} = \{60°, 200°\}$ with various data streams.

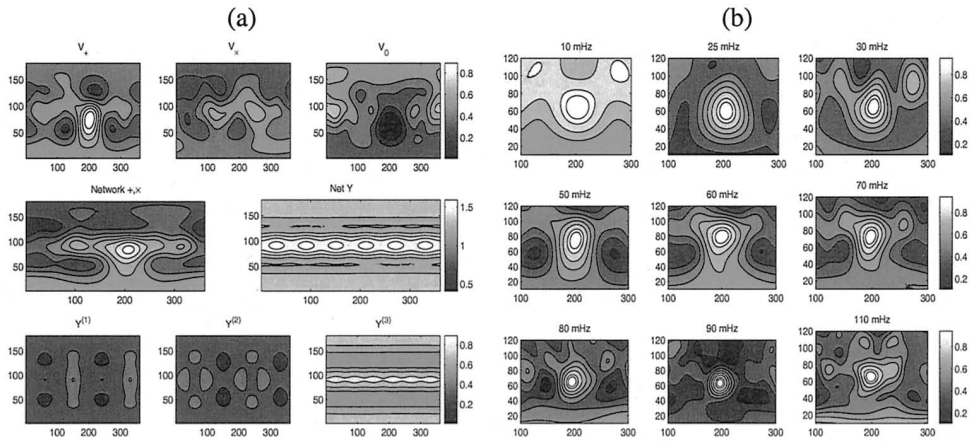

FIGURE 5. Tracking $\{\theta_B, \phi_B\} = \{60°, 200°\}$: Integrated squared SNR (a) at $f = 50$ mHz for various data streams, (b)for v_+ at different frequencies.

the features of Fig. 6: At low frequencies (< 25 mHz), the overall beam-width of v_+ decreases monotonically and is dominated by $Y^{(1,2)}$. At frequencies above 25 mHz, one observes modulation pattern in the beam-width (with frequency f_L). More importantly, at $f \sim nf_L$, $Y^{(3)}$ contributes a large fraction to SNR_+ as compared to the other two Y's, see Fig.3(a). Hence, the beam-width of v_+ is expected to carry the features of $Y^{(3)}$.

As we know, $Y^{(3)}$ is completely symmetric between the 3 arms. Its angular response is insensitive in the neighborhood of LISA's zenith as well as its equatorial plane whereas it is sensitive in the polar window of $\theta_L : \{30°, 60°\}$. A source at $\theta_B = 90°$ follows

a circular track in LISA sky with $\theta_L = 60°$, see Fig.2(a). Hence, the source's track coincides with the sensitive part of $Y^{(3)}$ beam-pattern which explains its maximum integrated sensitivity along $\theta_B = 90°$. As frequency increases, especially near $f = nf_L$, due to the symmetry of $Y^{(3)}$, for all θ_L, the integrated antenna pattern of $Y^{(3)}$ becomes invariant to azimuth ϕ_B, see Fig.4(b),5(a) which results in increase in the beam-width. This explains the sudden increase of solid angle at nf_L in Fig.6.

From Fig.6, one can estimate the number of non-overlapping patches (templates) required to cover the entire sky. For instance, at $f \sim 10$ mHz, one requires 20 such patches whereas at $f = 30$ mHz, this number goes to 60.

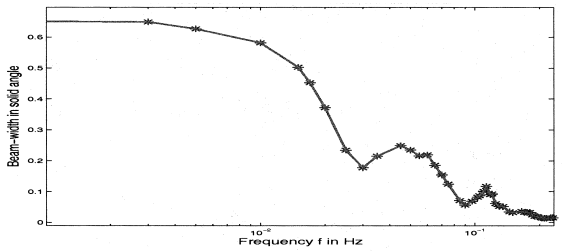

FIGURE 6. Tracking $\{\theta_B, \phi_B\} = \{60°, 200°\}$ with v_+: beam-width (obtained at 90% level) *vs* f.

4. CONCLUSIONS

In this work, we have studied the beaming properties of directionally optimal data streams v_+,$v_\times$ and v_0 which contain the complete information of the GW signal in a particular direction. We have shown that they are beamed (after tracking the source for a year) and could be useful in eliminating certain sky directions or for consistency checks in LISA data analysis.

5. ACKNOWLEDGEMENT

Thanks to Y. Chen, S.V. Dhurandhar, K. R. Nayak, J. Romano, L. Wen for useful comments. This work is supported by the Alexander von Humboldt Foundation's Sofja Kovalevskaja Programme (Funded by the German Ministry of Education and Research).

REFERENCES

1. P. Bender *et al.* "LISA: A Cornerstone Mission for the Observation of Gravitational Waves", System and Technology Study Report ESA-SCI(2000) 11, 2000.
2. K. Rajesh Nayak, S. V. Dhurandhar, A. Pai, J-Y Vinet, Phys. Rev.D 68 (2003) 122001.
3. M. Tinto, S. V. Dhurandhar, *Living Rev.Rel.* **8** (2005) 4.
4. T. Prince, M. Tinto and S. Larson, Phys. Rev. **D 66**, 122002 (2002), K. Rajesh Nayak, A. Pai, S. V. Dhurandhar and J-Y. Vinet, *Class. Quantum Grav*, **20,** 1217(2003).